Turkish Journal of Electrical Engineering & Computer Sciences

http://journals.tubitak.gov.tr/elektrik/

Research Article

Turk J Elec Eng & Comp Sci
(2024) 32: 21 – 33

doi:10.55730/1300-0632.4053

Error performance enhancement and complexity reduction in OFDM systems via coordinate interleaving under practical impairments

Mustafa Anıl REŞAT [1,*], **Armed TUSHA**[2], **Seda DOĞAN TUSHA**[2], **Serdar ÖZYURT**[1], **Hüseyin ARSLAN**[2]

[1]Department of Electrical and Electronics Engineering, Ankara Yıldırım Beyazıt University, Ankara, Turkiye

[2]Department of Electrical and Electronics Engineering, İstanbul Medipol University, İstanbul, Turkiye

Received: 09.04.2023 • **Accepted/Published Online:** 06.11.2023 • **Final Version:** 07.02.2024

Abstract: In this work, subcarrier coordinate interleaving (CI) is implemented to orthogonal frequency division multiplexing (OFDM) systems with the aim of both enhancing the error performance and reducing the implementation complexity. To this end, the modulated symbols are independently chosen from a modified M-ary amplitude-shift keying signal constellation under a specific CI strategy. In addition to doubling the diversity level of the original OFDM scheme, the adopted CI approach also drastically reduces the inverse fast Fourier transform (IFFT) size at the transmit side by guaranteeing the first half of the input vector to be identical with the second half at the input to the IFFT block. It is further demonstrated that the proposed system has the ability to enhance the robustness against common practical impairments such as insufficient cyclic prefix and phase noise. The closed-form expression of symbol error probability of the system is derived and confirmed with the simulation results.

Key words: Orthogonal frequency division multiplexing, signal space diversity, coordinate interleaving, intersymbol interference, phase noise

1. Introduction

Orthogonal frequency division multiplexing (OFDM) has been the keystone of modern communication standards such as digital audio and video broadcasting (DAB/DVB), IEEE 802.11, IEEE 802.16, and long-term evolution (LTE) [1–3]. Despite many strong waveform candidates like filter-bank multicarrier and generalized frequency division multiplexing, OFDM with numerology has also been selected as the basis of the 5G New Radio (5G-NR) technology. This interest can mainly be attributed to OFDM's resilience against frequency-selective fading and its ease of integration with multiple-input multiple-output systems, which is a valuable asset for the enhanced Mobile Broadband (eMBB) services [4–6]. OFDM assigns each subcarrier a portion of the channel spectrum that is narrower than the coherence bandwidth of the channel. This process is carried out such that subcarriers overlap each other in an orthogonal and spectrally efficient fashion. Despite the aforementioned advantages, OFDM is quite sensitive against any slight loss of orthogonality among the subcarriers such that symbol timing offset (STO) and carrier frequency offset (CFO) may cause substantial error performance degradation [7–14]. In [7], an analysis of OFDM systems under intercarrier interference (ICI) and intersymbol interference

*Correspondence: maresat@ybu.edu.tr

(ISI) is performed for time-invariant channels. Considering massive machine-type communications (mMTC), OFDM with index modulation (IM) is suggested in [8] to mitigate the effects of ICI induced by asynchronous transmission in uncoordinated mMTC networks. In [9], different types of OFDM frequency-domain IM strategies are compared with respect to their performances under CFO and in-phase/quadrature (IQ) imbalance.

In the literature, various approaches have been discussed to control and mitigate the impact of time-frequency constraints in OFDM-based systems. The most frequently used technique is adding a cyclic prefix (CP) to each OFDM symbol, with a length longer than or equal to the delay spread of a multipath channel. This CP helps eliminate ISI and transforms the relationship between the transmitted signal and the channel impulse response into a circular convolution operation. However, in applications like high-definition television broadcasting (HDTV) and satellite OFDM systems, where very long delay spreads may occur, the probability of the channel length exceeding the CP length increases [10]. Furthermore, despite a sufficient CP length, STO can induce ISI along with ICI. In [11], a fully asynchronous spatially multiplexed OFDM system is analyzed under different STO and CFO values. For over doubly dispersive channels, Taubock [12] proposed a low-complexity ICI/ISI equalizer for multicarrier models. Wang [13] presented an iterative method to subtract pseudonoise sequence padding for time-domain synchronous OFDM systems, mitigating ISI. An iterative algorithm, utilizing comb-type pilot signals, was demonstrated to weaken ICI and estimate channel gains for an OFDM mobile downlink communication system [14].

The instabilities within the transmitter/receiver oscillators lead to phase noise (PN) in a random time-varying fashion and cause unwanted modulation of the carrier signal's phase [15]. PN severely affects OFDM systems by destroying the orthogonality between the subcarriers. Two main detrimental effects introduced by PN on OFDM signals are common phase error (CPE) and ICI. The CPE component of PN causes all subcarriers to experience phase rotation that remains constant within an OFDM symbol period. On the other hand, the time-varying frequency-dependent part of PN causes ICI and acts like noise, bringing out different interference terms to different subcarriers during the transmission of an OFDM symbol. In [16], the effect of PN on an OFDM system is analyzed, and a mitigation method is proposed. A millimeter-wave OFDM experimental system that uses an iterative scheme to combat the impact of PN is studied in [17]. The work in [18] introduces a method that initially estimates the channel coefficients together with CPE and then cancels ICI. In [19], the effects of STO, CFO, and PN in OFDM and generalized frequency division multiplexing systems are analyzed in a comparative fashion under distinct scenarios. The joint PN, IQ imbalance, and frequency offset estimation along with a low-complexity mitigation method are discussed in [20].

Diversity techniques generally require the consumption of additional resources reserved for statistically independent copies of the transmitted signals. Conventional diversity approaches rely on the extra utilization of time, frequency, code, and space dimensions. On the other hand, signal space diversity (SSD) is a low-complexity diversity method that improves the error performance of a system by only exploiting the inherent orthogonality within the signal space composed of the modulated symbols [21]. To increase diversity for a system based on two-dimensional modulation, SSD initially introduces a rotation on the original constellation diagram so that all the signal points have distinct I and Q components. The rotation angle is usually selected such that the error probability is minimized [22, 23]. Subsequently, the I and Q components of a symbol are sent via different channel realizations by virtue of coordinate interleaving (CI). The CI scheme is commonly arranged according to a specific strategy that also optimizes error performance [24, 25].

OFDM and SSD have been combined extensively in the literature. SSD is combined with bit-interleaved coded OFDM (BICM) technique under frequency-selective fading channels in [26]. BICM is applied among subcarriers in [27] where multiple transmit antennas are used for the transmission of symbols. A dynamic CI pattern is performed over some OFDM subcarriers with channel phases larger than a threshold level defined beforehand in [28]. To improve physical layer security, SSD is incorporated into a single-antenna OFDM system in [29] and into an Alamouti multiple-input single-output system in [30]. OFDM is also used along with a well-known SSD technique called constellation rotation and cyclic Q delay in [31].

In this study, we consider an application of SSD to OFDM systems and propose the utilization of a modified M-ary amplitude-shift keying (M-ASK) modulation scheme under a particular subcarrier CI strategy based on [24]. To exploit SSD, we first rotate the one-dimensional M-ASK scheme and enable the signal points to have distinct I and Q components. Subsequently, the I and Q components of the chosen symbol are transmitted from different subcarrier channels. It is demonstrated that this model introduces diversity gain into the system and significantly improves the error performance under insufficient CP and PN. The proposed CI strategy also substantially reduces the system complexity at the transmitter by decreasing the computational load involved in the inverse fast Fourier transform (IFFT) operation to less than half of conventional OFDM-based systems. To the best of our knowledge, fine-tuning the CI pattern as if both the error rate and IFFT complexity decline has not been studied yet in the literature. Furthermore, the closed-form expression of the symbol error probability for the proposed scheme is analytically derived and corroborated by the simulation results.

Throughout this work, the operators $\mathbb{E}\{.\}$, $|.|$, $(.)^*$, j, $\mathcal{O}(.)$, $\Re\{.\}$, $\Im\{.\}$ stand for the expectation, magnitude, complex conjugate, $\sqrt{-1}$, big O notation, real and imaginary parts of a complex number, respectively. The joint probability density function (PDF) of x and y is symbolized by $f(x,y)$.

2. System model

In this section, the system model of the proposed OFDM scheme with smart coordinate interleaving (OFDM-CI) is described. A scenario with no practical impairments is initially inspected. Following that, the system model under practical imperfections such as insufficient CP and PN is investigated. It should be noted that the OFDM symbol index i is only depicted in subsection 2.2 for the sake of simplicity.

2.1. OFDM-CI system model

In this work, an OFDM-CI model that transmits N (a power of two) symbols via N subcarriers during an OFDM frame period is considered. It is pretended that the channel characteristics do not change within the OFDM symbol period and independently change between consecutive transmissions. The number of total resolvable multipaths is shown with L ($L << N$). The channel state information only exists at the receive side. Figure 1 shows the block diagrams of the transmit and receive side schemes for the system model.

The modulated symbols $\{s_1, s_2, ..., s_N\}$ are independently drawn from an M-ASK signal constellation rotated by an angle of $\pi/4$ counter-clockwise. We assume that the average symbol energy is constrained by E_s. We have $s_k = s_{kI} + js_{kQ}$ for $k \in \{1, 2, ..., N\}$ where s_{kI} and s_{kQ} represent the I and Q components of the k-th modulated symbol, respectively. CI is applied on the sequence $\{s_1, s_2, ..., s_N\}$ before the inverse FFT (IFFT) block to produce $\{X_1, X_2, ..., X_N\}$. Here, $X_k = s_{\alpha I} + js_{\beta Q}$ for $\alpha, \beta \in \{1, 2, ..., N\}$ such that $\alpha \neq \beta$. The values of subcarrier indices α and β are fine-tuned according to a specific interleaving strategy. To optimize error performance, the CI strategy in our work is chosen such that the correlation coefficient between any two

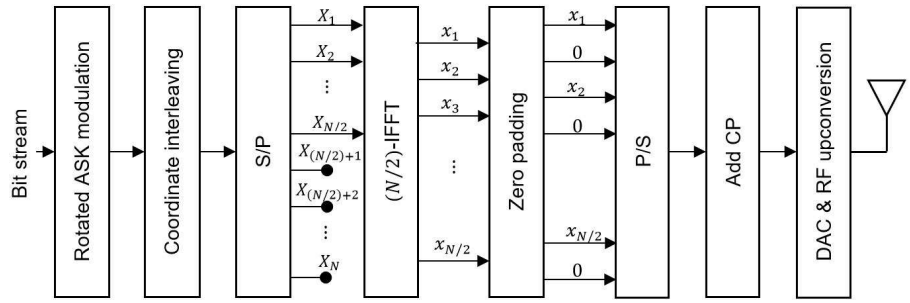

(a) Transmitter

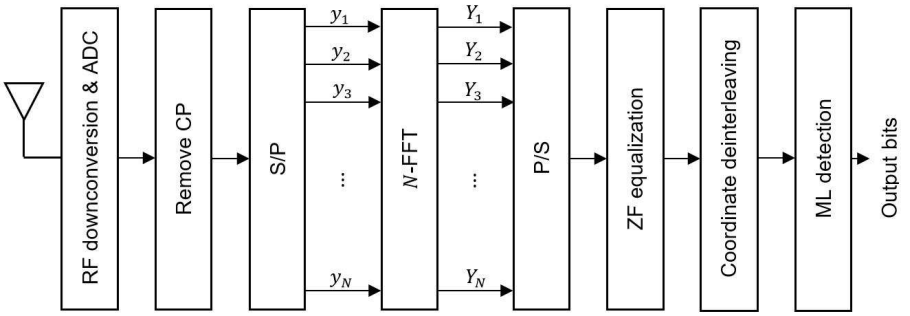

(b) Receiver

Figure 1. Block diagram of reduced complexity OFDM with smart subcarrier CI.

distinct subcarrier channel gains affecting the I and Q components of a modulated symbol equal to zero. To this end, one of the CI procedures introduced in [24] is adopted such that $(\alpha - \beta)$ is equal to $N/2$. This can be expressed as follows

$$X_k = \begin{cases} s_{kI} + js_{(k+N/2)I} & \text{for } 1 \le k \le N/2, \\ s_{(k-N/2)Q} + js_{kQ} & \text{for } N/2+1 \le k \le N. \end{cases} \tag{1}$$

Note that any modulated symbol has identical I and Q coordinates thanks to the employed rotation on the original signal set. Thus, the first half of the $\{X_1, X_2, ..., X_N\}$ equals the second half, i.e. a repetition in the frequency domain exists. Assume that the sequence $\{x_1, x_2, x_3, x_4, ..., x_{N-1}, x_N\}$ denotes the IFFT of $\{X_1, X_2, ..., X_N\}$. It is straightforward to show that the baseband time samples with even subcarrier indices are equal to zero and the remaining samples can be obtained from the IFFT of the first (or second) half of $\{X_1, X_2, ..., X_N\}$. After applying an $(N/2)$-IFFT operation to $\{X_1, X_2, ..., X_{N/2}\}$ which generates $\{x_1, x_3, x_5, ..., x_{N/2}\}$, a single zero is padded in between each signal sample to obtain the whole set of baseband time samples of N size. Subsequently, a cyclic prefix of length G is inserted to the start of the baseband time samples. After the digital-to-analog conversion (DAC) operation, time-domain signal x_n passes through the multipath channel h_n. The channel model is presumed to be a multipath frequency-selective Rayleigh fading channel with taps of $\{h_0, h_1, ..., h_{L-1}\}$. Here, h_l for $l \in \{0, 1, ..., L-1\}$ are independent and identically distributed (i.i.d) zero-mean complex Gaussian random variables with $E\{|h_l|^2\} = 1/L$. The received signal is given by

$$y_n = h_n \circledast x_n + z_n, \tag{2}$$

where $\circledast$ denotes circular convolution. We first investigate the scenario with perfect synchronization and then

consider the case with practical imperfections at the receiver. Let the symbol sequence obtained after analog-to-digital conversion (ADC), CP removal, and N-FFT operations at the receive side be shown as $\{Y_1, Y_2, ..., Y_N\}$. Then, we can write

$$Y_k = H_k X_k + Z_k, \tag{3}$$

where the channel gains of the subcarriers $H_k = \sum_{l=0}^{L-1} h_l e^{-j2\pi kl/N}$ for $k \in \{1, 2, ..., N\}$ are zero-mean complex Gaussian random variables with $E\{|H_k|^2\} = 1$. Also, Z_k for $k \in \{1, 2, ..., N\}$ stands for i.i.d zero-mean complex Gaussian noise terms each with a variance of $N_0/2$ per dimension. At the receiver, with the application of zero-forcing equalization on Y_k, we get $\hat{Y}_k = (H_k^*/|H_k|)Y_k = |H_k|X_k + \hat{Z}_k$ where $\hat{Z}_k = (H_k^*/|H_k|)Z_k$ for $k \in \{1, 2, ..., N\}$. After using coordinate deinterleaving (CD), the maximum likelihood (ML) detector forms the decision variable for the k-th modulated symbol s_k as

$$d_k = \Re\{\hat{Y}_\alpha\} + j\Im\{\hat{Y}_\beta\} = |H_\alpha| s_{kI} + j|H_\beta| s_{kQ} + \hat{Z}_k, \tag{4}$$

where $\hat{Z}_k$ shares the same statistics as Z_k and represents the noise term after CD. In addition, we have

$$\{\alpha, \beta\} = \begin{cases} k, k + N/2 & \text{for } 1 \le k \le N/2, \\ k - N/2, k & \text{for } N/2 + 1 \le k \le N, \end{cases} \tag{5}$$

which are utilized to detect the information carried by s_k.

2.2. Interference formulation for insufficient CP length

An interference-free signal can be received for OFDM if the time spread of the channel does not exceed the CP duration. Otherwise, if the CP length is shorter than the channel spread, ISI and ICI appear, affecting the received symbol corresponding to the k-th subcarrier within the i-th OFDM symbol as follows

$$Y_{i,k} = H_{i,k} X_{i,k} + I_{i,k}^{ICI} + I_{i,k}^{ISI} + Z_{i,k}, \tag{6}$$

where $I_{i,k}^{ICI}$ and $I_{i,k}^{ISI}$ represent the intercarrier interference and intersymbol interference, respectively. In general, after discarding the CP, the n-th sample of the received time domain signal equals

$$y_{i,n} = \sum_{l=0}^{L-1} h_{i,l} x_{i,(n-l)_N} u_{n-l+G} + \sum_{l=G}^{L-1} h_{i-1,l} x_{i-1,(n-l+G)_N} [1 - u_{n-l+G}] + z_{i,n}, \tag{7}$$

where $(\xi)_N$ is the residue ξ of modulo N and u_n denotes the step function with $u_n = 1$ if $n \ge 0$, else $u_n = 0$. The term $x_{i-1,n}$ denotes the previous consecutive OFDM symbol regarding $x_{i,n}$. For simplicity, Figure 2 illustrates the scenario of an OFDM signal with insufficient CP. After applying the FFT transform, the mathematical representation of the received signal at k-th subcarrier is given as follows

$$\begin{aligned} Y_{i,k} &= H_{i,k} X_{i,k} + Z_{i,k} \\ &+ \sum_{l=D}^{L-1} h_{i,l} \sum_{v=0, v\neq k}^{N-1} \frac{1}{N} X_{i,v} e^{\frac{-j2\pi vl}{N}} \sum_{n=l-G}^{N-1} e^{\frac{j2\pi n(v-k)}{N}} + \sum_{l=G}^{L-1} h_{i-1,l} \sum_{v=0, v\neq k}^{N-1} \frac{1}{N} X_{i-1,v} e^{\frac{j2\pi v(G-l)}{N}} \sum_{n=0}^{l-G-1} e^{\frac{j2\pi n(v-k)}{N}}, \end{aligned} \tag{8}$$

where the third and fourth terms of the equation determine $I_{i,k}^{ICI}$ and $I_{i,k}^{ISI}$, respectively.

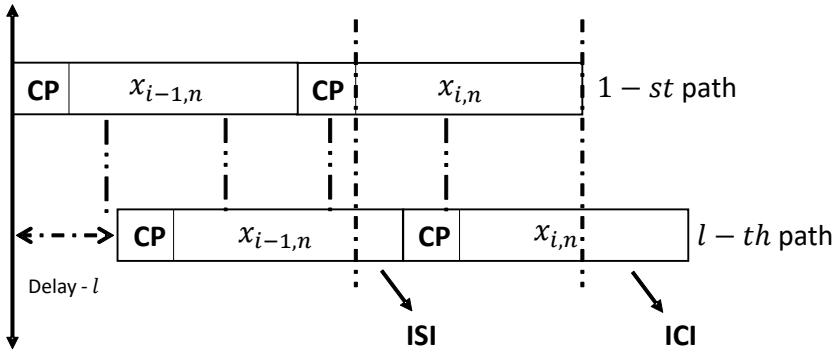

Figure 2. ISI and ICI due to insufficient CP length.

2.3. Effect of phase noise on the received signal

The impact of PN can be modeled as a random noise term that acts upon the received signal as an exponential multiplication. Therefore, the n-th sample of the received signal under PN can be shown in the time domain as $\tilde{y}_n = y_n e^{j\eta_n}$ where η_n is the random PN term that rotates y_n. To simplify the analysis, it is generally pretended that the noise term is much smaller than 1, i.e., $e^{j\eta_n} \approx 1 + j\eta_n$ [32]. As a result, the received symbol corresponding to the k-th subcarrier under PN transforms into

$$\tilde{Y}_k \approx H_k X_k \frac{1}{N}\sum_{n=0}^{N-1}(1+j\eta_n) + \frac{1}{N}\sum_{v=0,v\neq k}^{N-1} H_v X_v \sum_{n=0}^{N-1}(1+j\eta_n)e^{\frac{-j2\pi n(k-v)}{N}} + Z_k. \tag{9}$$

Here, the first term is the CPE and causes an equal amount of rotation on each subcarrier. The second term on the other hand is the ICI which arises because of the loss of orthogonality and shows the distorting effect of Y_v on Y_k for $v \neq k$.

3. Theoretical analysis

In the following, a mathematical study that involves error probability, diversity, and complexity analyses of the proposed scheme is presented.

3.1. Error probability analysis

Let $\gamma_k = |H_k|^2$ for $k \in \{1, 2, \ldots, N\}$. Using a similar approach to that in [24], it is straightforward to conclude that all the modulated symbols have the identical average symbol error probability (SEP). The proposed CI strategy enables to have the same joint PDF for any subcarrier pair. Therefore, after some elaboration, the unconditional (overall) SEP can be written as follows:

$$P(e) = \frac{2(M-1)}{M}\mathbb{E}\left(\mathrm{Q}\left(\sqrt{\frac{E_s N(\gamma_{k\alpha}+\gamma_{k\beta})}{N_0(N+G)(\frac{2\sum_{m=1,3,5,\ldots}^{M} m^2}{M})}}\right)\right), \tag{10}$$

where M represents the modulation level and $\mathrm{Q}(x) = \frac{1}{\sqrt{2\pi}}\int_x^\infty \exp\left(-\frac{u^2}{2}\right) du$ [33]. Note that both $\gamma_{k\alpha}$ and $\gamma_{k\beta}$ are exponentially distributed random variables. Since the correlation coefficient between any subcarrier pairs is equal to zero under our CI strategy, the joint PDF of $\gamma_{k\alpha}$ and $\gamma_{k\beta}$ can be written as

$$P(e)=\frac{2}{\pi}\frac{(M-1)}{M}\int_0^{\pi/2}\int_0^{\infty}\int_0^{\infty}\exp\left(-\frac{E_sN\left(\gamma_{k\alpha}+\gamma_{k\beta}\right)}{2N_0\left(N+G\right)\left(\frac{2\sum_{m=1,3,5,\ldots}^{M}m^2}{M}\right)\sin^2\left(\phi\right)}\right)\exp\left(-\gamma_{k\alpha}-\gamma_{k\beta}\right)\,\mathrm{d}\gamma_{k\alpha}\mathrm{d}\gamma_{k\beta}\mathrm{d}\phi. \tag{12}$$

$$f(\gamma_{k\alpha},\gamma_{k\beta})=\exp(-\gamma_{k\alpha}-\gamma_{k\beta}), \tag{11}$$

for $\gamma_{k\alpha},\gamma_{k\beta}\geq 0$. Using Craig's formula [33], we can convert (10) into (12) as given at the top of the page.

Evaluating the inner integrals, (12) can be written as:

$$\mathrm{P}(e)=\frac{2}{\pi}\frac{(M-1)}{M}\int_0^{\pi/2}\left(\frac{\sin^2(\phi)}{\sin^2(\phi)+\psi}\right)^2 d\phi, \tag{13}$$

where $\psi=(E_sN)/\left\{2N_0(N+G)\left(\frac{2\sum_{m=1,3,5,\ldots}^{M}m^2}{M}\right)\right\}$. Using [33], an exact closed-form expression for the preceding integral can be attained as follows:

$$P(e)=\frac{2\,(M-1)}{M}\left(\frac{1-\sqrt{\frac{\psi}{\psi+1}}}{2}\right)^2\left[2+\sqrt{\frac{\psi}{\psi+1}}\right]. \tag{14}$$

3.2. Diversity analysis

In the limit as $E_s/N_0\to\infty$, it can be shown that

$$P(e)\approx\frac{2}{\pi}\frac{(M-1)}{M}\int_0^{\frac{\pi}{2}}\frac{1}{\left(\frac{\psi}{\sin(\phi)^2}\right)^2}d\phi\approx\left(\frac{E_s}{N_0}\right)^{-2}\frac{3(M-1)}{2M}\left(\frac{N}{2\left(N+G\right)\left(\frac{2\sum_{m=1,3,5,\ldots}^{M}m^2}{M}\right)}\right)^{-2}, \tag{15}$$

which implies that a diversity order of two is achieved.

3.3. Complexity analysis

The FFT algorithm enables the computation of an N point DFT operation with significantly reduced complexity. To calculate the N-DFT of a signal, N summation operations are applied for N output terms, resulting in a complexity of $\mathcal{O}\left(N^2\right)$. In contrast, the FFT operation reduces the complexity to $\mathcal{O}\left(N\log N\right)$. With a radix-2 FFT algorithm, there are $\log N$ stages of computation, and for each stage, there exist $N/2$ complex multiplication and N complex addition operations. A crucial aspect of our CI method is to reduce the required IFFT size, thereby significantly lowering the overall complexity. This reduction is attributed to the employed CI strategy, yielding a vector at the input to the IFFT block whose first half is identical to the second half. Consequently, it is possible to employ an $N/2$ point IFFT together with zero-padding to obtain the same output as in the original N-IFFT case. Ignoring the extra negligible complexity due to the zero-padding process, this process changes the complexity of the IFFT block from $\mathcal{O}\left(N\log N\right)$ to $\mathcal{O}\left(\frac{N}{2}\log\frac{N}{2}\right)$. For instance, the IFFT complexity scales down from $\mathcal{O}\left(896\right)$ to $\mathcal{O}\left(384\right)$ when $N=128$. It is noteworthy that the achieved gain in terms of complexity reduction increases as N gets larger.

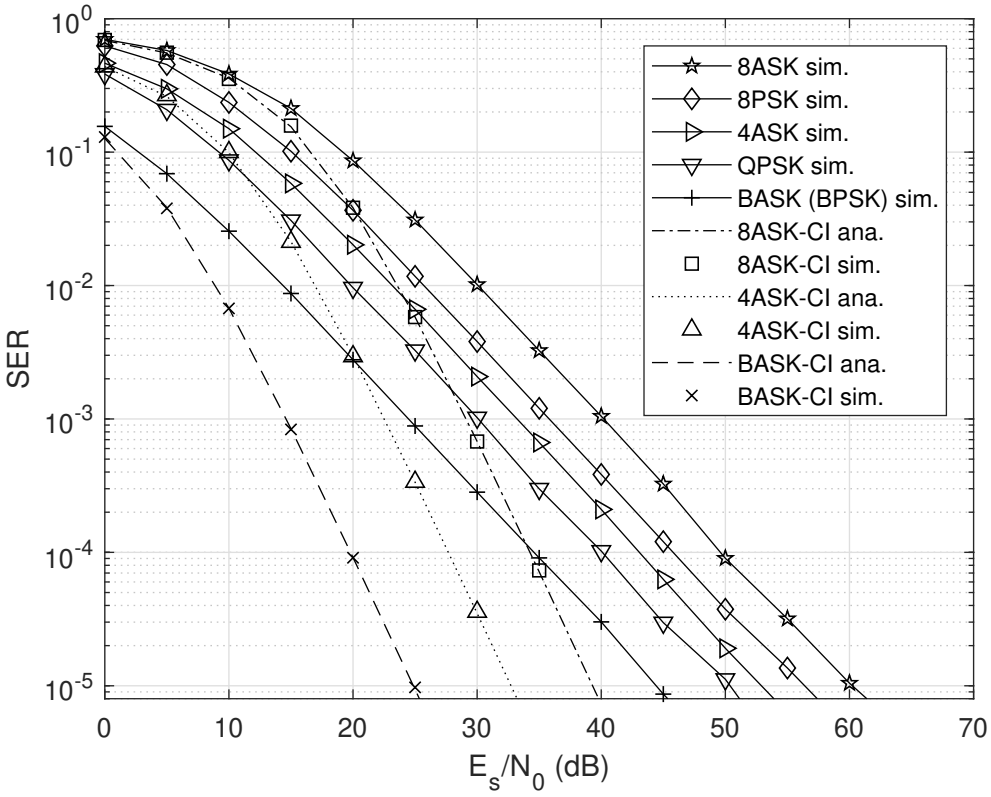

Figure 3. Error performance comparison under no synchronization imperfections for $M = 2$, 4, and 8.

4. Numerical results

In this section, Monte Carlo simulations are employed to evaluate the symbol error rate (SER) performance of the proposed OFDM-CI under insufficient CP and PN conditions.

Figure 3 illustrates the SER performance of the OFDM-CI system under no synchronization imperfections and a 10-tap frequency-selective fading channel, with $N = 128$ and $G = 16$. The results clearly indicate that the proposed CI method, along with M-ASK modulation schemes, outperforms the conventional OFDM system. It can be observed that for an SER of 10^{-4}, the suggested CI technique provides an approximate 14.9 dB signal-to-noise (SNR) gain with binary ASK (BASK) and roughly 15.3 dB extra SNR gains with 4ASK and 8ASK over the traditional OFDM approach. The proposed technique excels compared to conventional OFDM due to the CI strategy, eliminating the correlation between the gains of subcarrier channels transmitting the I and Q components of a specific symbol separately. Consequently, it is possible to both reduce the complexity of the transmit side and achieve a considerably lower SER simultaneously. As a reference point, the SER performance of the recommended model is also compared against their corresponding phase-shift keying (PSK) counterparts without CI, contributing approximately 14.9 dB, 12.2 dB, and 11.6 dB more SNR gains with BASK, 4ASK, and 8ASK, respectively, for an SER of 10^{-4}. Finally, the equivalent analytical and simulation results indicate the accuracy of the theoretical analysis given in Subsection 3.1.

Figures 4 and 5 provide the error rate of OFDM-CI under ISI and ICI induced by inadequate CP length, with $N = 128$ and $M = 2$, 4, 8. The proposed OFDM-CI offers better error performance than classical OFDM,

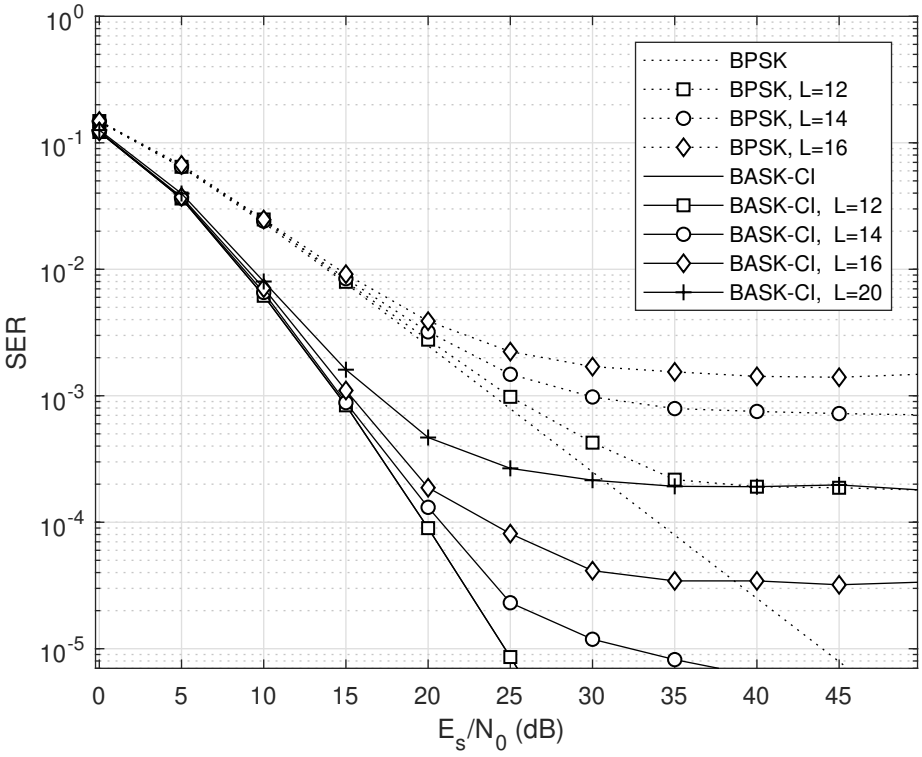

Figure 4. Error performance of M-ASK OFDM-CI vs M-PSK OFDM for $M = 2$ under insufficient CP ($G = 10$).

owing to not only the CI strategy but also its sparse structure. In other words, the sparse representation of the transmitted signal acts as guard time for $x_{i,n}$ and mitigates the channel effect. As shown in the figures, no interference occurs when the number of channel taps exceeds the CP size by 2 taps ($G = 10,\ L = 12$). However, the performance of classical OFDM saturates around 10^{-3} SER for $M = 2$ and ($G = 10,\ L = 12$). Although the impact of interference becomes significant as the difference between the number of channel taps and CP length increases, the effect of insufficient CP in OFDM-CI is less than that of OFDM due to zeros in $x_{i,n}$. In the case of ($G = 10,\ L = 14$), the error performance of OFDM-CI and OFDM saturates around 40 dB SNR and 35 dB SNR, respectively. On the other hand, OFDM-CI experiences the same saturation region (35 dB SNR) with OFDM under significant interference impact, as shown in the case of ($G = 10,\ L = 16$). In such a scenario, only the error performance gain introduced by the CI exists. The estimation of channel parameters is a time and economically costly process, always associated with some error. Fortunately, the OFDM-CI scheme can afford communication with reliability below 10^{-4} SER until a 10-tap difference exists between the channel length and the utilized CP size. On the other hand, no error is tolerated on the conventional OFDM side to satisfy this reliability constraint. Therefore, OFDM-CI can be considered to be a possible solution for various applications and use-cases with high subcarrier spacing (SCS) in 5G-NR. Since CP size linearly decreases with the increase of SCS, the immunity of OFDM-CI against insufficient CP can be utilized in 5G and beyond wireless systems.

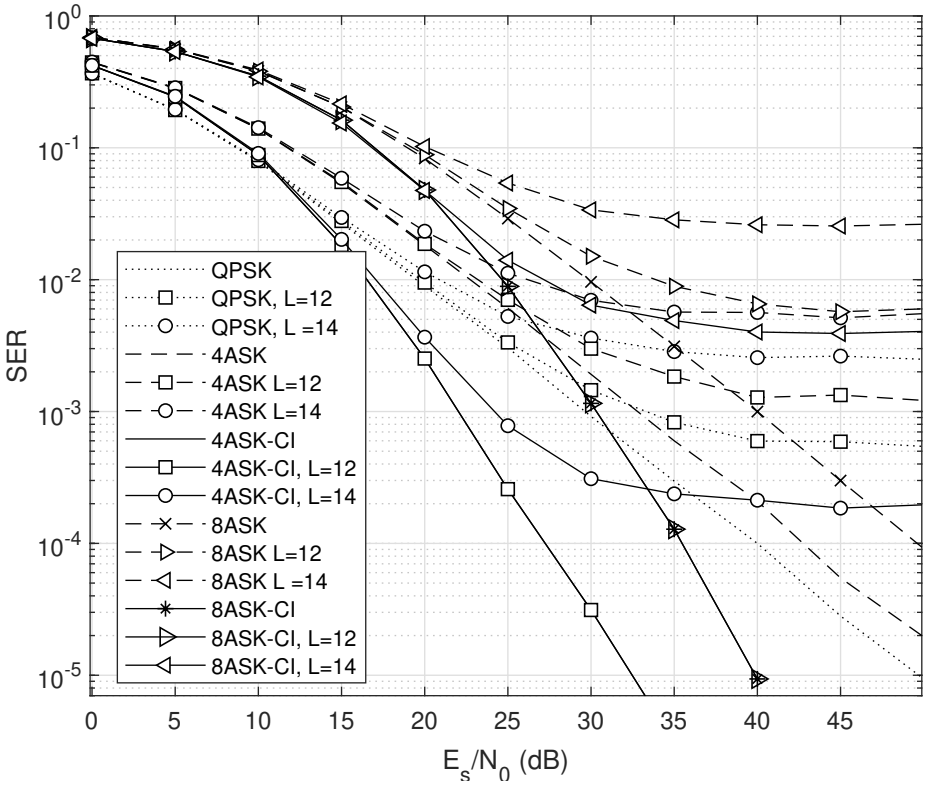

Figure 5. Error performance of M-ASK OFDM-CI vs M-PSK OFDM for $M = 4$, 8 under insufficient CP ($G = 10$).

Finally, the impact of PN on the error performance of the proposed model is analyzed for $\eta = 5°$ in Figure 6, with $N = 128$, $G = 16$, and $L = 10$. The OFDM-CI model is capable of substantially lowering the inevitable error floor due to PN compared with the regular OFDM system. For $\eta = 5°$, the CI technique reduces the error floor for all three modulation levels, e.g., from $1.1\text{x}10^{-3}$ to 10^{-5} for 4-ASK and from $5\text{x}10^{-3}$ to $2.8\text{x}10^{-4}$ for 8-ASK, approximately. Similarly, the suggested OFDM-CI model provides significantly lower error floors when compared with the conventional OFDM scheme with PSK for each of the three modulation levels. This reduction ranges roughly from $5.5\text{x}10^{-4}$ to 10^{-5} for quadrature PSK (QPSK) and from $2\text{x}10^{-3}$ to $2.8\text{x}10^{-4}$ for 8-PSK. Therefore, the suggested model can be considered a viable alternative to complex and costly PN suppression methods.

5. Conclusion

This study proposes a novel application of CI in OFDM schemes to enhance the system against two common practical impairments; PN and insufficient CP leading to ISI and ICI effects. With the aid of a smart CI strategy ensuring uncorrelated channel gains between the subcarriers carrying the I and Q components of a sent symbol, it is demonstrated that the SER performance can be significantly improved. Additionally, the applied CI policy reduces the overall complexity of the transmitter substantially by enabling a reduced-size IFFT operation. The introduced method in this paper can be integrated into multiple-antenna schemes. Moreover, the complexity reduction feature at the transmit side makes this method particularly attractive for future studies involving multiple-user uplink scenarios with battery-limited power at the user terminals. The proposed system model

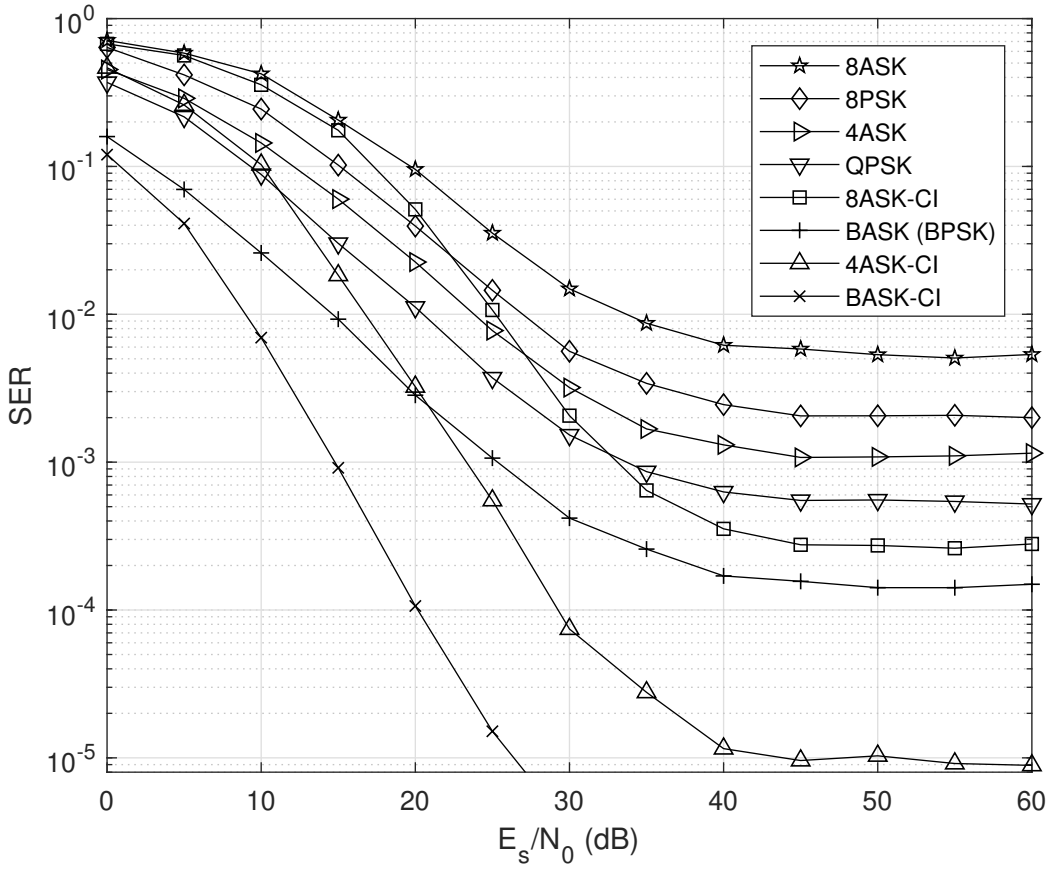

Figure 6. Error performance comparison under $\eta = 5^\circ$ for $M = 2$, 4 and 8.

can also be employed with the recently introduced orthogonal time-frequency space modulation over high-mobility channels. A complexity reduction can be obtained regarding the inverse symplectic finite Fourier transform block at the transmit side, representing a promising avenue for future work.

References

[1] Farhang-Boroujeny B, Moradi H. OFDM inspired waveforms for 5G. IEEE Communications Surveys & Tutorials 2016; 18 (4): 2474-2492. https://doi.org/10.1109/COMST.2016.2565566

[2] Acar Y, Çolak SA, Başar E. Channel estimation for OFDM-IM systems. Turkish Journal of Electrical Engineering and Computer Sciences 2019; 27 (3): 1908–1921. https://doi.org/10.3906/elk-1803-101

[3] Van Zelst A, Schenk TCW. Implementation of a MIMO OFDM-based wireless LAN system. IEEE Transactions on Signal Processing 2004; 52 (2):483-494. https://doi.org/10.1109/TSP.2003.820989

[4] Lien S, Shieh S, Huang Y, Su B, Hsu Y, Wei H. 5G new radio: Waveform, frame structure, multiple access, and initial access. IEEE Communications Magazine 2017; 55 (6): 64-71. https://doi.org/10.1109/MCOM.2017.1601107

[5] Lin H. Flexible configured OFDM for 5G air interface. IEEE Access 2015; 3: 1861-1870. https://doi.org/10.1109/ACCESS.2015.2480749

[6] Seyman MN, Taşpınar N. Symbol detection using the differential evolution algorithm in MIMO-OFDM systems. Turkish Journal of Electrical Engineering and Computer Sciences 2013; 21 (2): 373-380. https://doi.org/10.3906/elk-1103-16

[7] Nguyen V, Kuchenbecker H. Intercarrier and intersymbol interference analysis of OFDM systems on time-invariant channels. In: The 13^{th} IEEE International Symposium on Personal, Indoor and Mobile Radio Communications; Lisboa, Portugal; 2002. pp. 1482-1487.

[8] Doğan S, Tusha A, Arslan H. OFDM with index modulation for asynchronous mMTC networks. Sensors 2018; 18 (4). https://doi.org/10.3390/s18041280

[9] Tusha A, Doğan S, Arslan H. Performance analysis of frequency domain IM schemes under CFO and IQ imbalance. In: IEEE 30^{th} Annual International Symposium on Personal, Indoor and Mobile Radio Communications (PIMRC); Istanbul, Turkey; 2019.

[10] Chen S, Zhu C. ICI and ISI analysis and mitigation for OFDM systems with insufficient cyclic prefix in time-varying channels. IEEE Transactions on Consumer Electronics 2004; 50 (1): 78-83. https://doi.org/10.1109/TCE.2004.1355879

[11] Kotzsch V, Fettweis G. Interference analysis in time and frequency asynchronous network MIMO OFDM systems. In: IEEE Wireless Communication and Networking Conference; Sydney, Australia; 2010.

[12] Taubock G, Hampejs M, Svac P, Matz G, Hlawatsch F, Grochenig K. Low-complexity ICI/ISI equalization in doubly dispersive multicarrier systems using a decision-feedback LSQR algorithm. IEEE Transactions on Signal Processing 2011; 59 (5): 2432-2436. https://doi.org/10.1109/TSP.2011.2113181

[13] Wang J, Yang Z, Pan C, Song J, Yang L. Iterative padding subtraction of the PN sequence for the TDS-OFDM over broadcast channels. IEEE Transactions on Consumer Electronics 2005; 51 (4): 1148-1152. https://doi.org/10.1109/TCE.2005.1561837

[14] Hijazi H, Ros L. Rayleigh time-varying channel complex gains estimation and ICI cancellation in OFDM systems. European Transactions on Telecommunications 2009; 20: 782-796. https://doi.org/10.1002/ett.1366

[15] Armada AG. Understanding the effects of phase noise in orthogonal frequency division multiplexing (OFDM). IEEE Transactions on Broadcasting 2001; 47 (2): 153-159. https://doi.org/10.1109/11.948268

[16] Wu S, Bar-Ness Y. OFDM systems in the presence of phase noise: consequences and solutions. IEEE Transactions on Communications 2004; 52 (11):1988-1996. https://doi.org/10.1109/TCOMM.2004.836441

[17] Shin D, Suyama S, Suzuki H, Fukawa K. 10 Gbps millimeter-wave OFDM experimental system with iterative phase noise compensation. In: 2013 IEEE Radio and Wireless Symposium; Austin, TX, 2013. pp. 184-186.

[18] Munier F, Eriksson T, Svensson A. An ICI reduction scheme for OFDM system with phase noise over fading channels. IEEE Transactions on Communications 2008; 56 (7): 1119-1126. https://doi.org/10.1109/TCOMM.2008.050063

[19] Lim B, Ko Y. SIR analysis of OFDM and GFDM waveforms with timing offset, CFO, and phase noise. IEEE Transactions on Wireless Communications 2017; 16 (10): 6979-6990. https://doi.org/10.1109/TWC.2017.2736998

[20] Tubbax J, Van der Perre L, Donnay S, Engels M, Moonen M, Man H. Joint compensation of IQ imbalance, frequency offset and phase noise in OFDM receivers. European Transactions on Telecommunications 2004; 15 (3): 283-292. http://dx.doi.org/10.1002/ett.974

[21] Boutros J, Viterbo E. Signal space diversity: a power- and bandwidth-efficient diversity technique for the Rayleigh fading channel. IEEE Transactions on Information Theory 1998; 44 (4):1453-1467. https://doi.org/10.1109/18.681321

[22] Resat MA, Cicek A, Özyurt S, Cavus E. Analysis and FPGA implementation of zero-forcing receive beamforming with signal space diversity under different interleaving techniques. Journal of Circuits, Systems and Computers 2020; 29 (1). https://doi.org/10.1142/S0218126620500073

[23] Xie Q, Song J, Peng K, Yang F, Wang Z. Coded modulation with signal space diversity. IEEE Transactions on Wireless Communications 2011; 10 (2): 660-669. https://doi.org/10.1109/TWC.2011.120810.100951

[24] Özyurt S, Kucur O. Performance of OFDM with signal space diversity using subcarrier coordinate interleaving. IEEE Transactions on Vehicular Technology 2018; 67 (10): 10134-10138. https://doi.org/10.1109/TVT.2018.2864645

[25] Yusuf M, Arslan H. On signal space diversity: An adaptive interleaver for enhancing physical layer security in frequency selective fading channels. Physical Communication 2017; 24: 154-160. https://doi.org/10.1016/j.phycom.2017.07.001

[26] Tran NH, Nguyen HH, Le-Ngoc T. Bit-interleaved coded OFDM with signal space diversity: subcarrier grouping and rotation matrix design. IEEE Transactions on Signal Processing 2007; 55 (3): 1137-1149. https://doi.org/10.1109/TSP.2006.887107

[27] Rende D, Wong TF. Bit-interleaved space-frequency coded modulation for OFDM systems. IEEE Transactions on Wireless Communications 2005; 4 (5): 2256-2266. https://doi.org/10.1109/TWC.2005.853816

[28] Li H, Wang X, Zou Y. Dynamic subcarrier coordinate interleaving for eavesdropping prevention in OFDM systems. IEEE Communications Letters 2014; 18 (6): 1059-1062. https://doi.org/10.1109/LCOMM.2014.2315648

[29] Li H, Wang X, Tang H. Compensation of imperfect channel reciprocity through MMSE prediction for physical-layer confidentiality enhancement. In: International Conference on Military Communications and Information Systems (ICMCIS); Brussels, Belgium, 2016.

[30] Resat MA, Karakoc MC, Özyurt S. Improving physical layer security in Alamouti OFDM systems with subcarrier coordinate interleaving. IET Communications 2020; 14 (16): 2687-2693. https://doi.org/10.1049/iet-com.2019.0542

[31] Tomasin S, Butussi M. Low complexity demapping of rotated and cyclic Q delayed constellations for DVB-T2. IEEE Wireless Communications Letters 2012; 1 (2): 81-84. https://doi.org/10.1109/WCL.2012.012012.110260

[32] Robertson P, Kaiser S. Analysis of the effects of phase-noise in orthogonal frequency division multiplex (OFDM) systems. In: Proceedings IEEE International Conference on Communications; Seattle, WA, 1995. pp. 1652-1657.

[33] Simon AK, Alouini MS. Digital Communication over Fading Channels: A Unified Approach to Performance Analysis. John Wiley & Sons, 2000.